# Chapter 1

# Astronomical Calibration Mission Study

This chapter describes the design and development activities that are undertaken in order to determine the feasibility of the AstroCal mission using a Generic Nanosatellite Bus (GNB) platform. Section 1.1 provides an introduction to AstroCal mission background, and the GNB form factor. Section 1.2 lists the expected deliverables by the end of this mission study. Section 1.3 describes how the GNB platform is adapted to the AstroCal mission, based on the mission requirements as well as the constraints imposed by the payload subsystem. Section 1.4 describes the design and development of the payload subsystem, from conceptualization to preliminary design. In Section 1.5, the AstroCal spacecraft system level mass budget is presented in details. Lastly, in Section 1.6, the conclusions of this study along with the recommendations for future work are provided.

## 1.1 Introduction

The AstroCal mission study by SFL is an extension to the Airborne Laser for Telescopic Atmospheric Interference Reduction (ALTAIR) project that is undertaken by the Department of Physics and Astronomy at University of Victoria (UVic). Since early 2010, UVic has been running a series of experiments that are intended to calibrate ground telescopes using airborne lasers (carried by high-altitude balloons). The main objective of these experiments has been to develop tools and techniques for in-situ characterization of optical losses due to the Earth's atmosphere and optics in telescopes. Among others, a limiting factor in balloon experiments is the inability to reach very high altitudes below which the entire Earth's atmosphere lies. This is critical since supernovae and stars that are observed by ground telescopes are clearly well beyond Earth's atmosphere. The light

arriving at Earth from these terrestrial bodies , therefore, gets fully attenuated as it travels through the Earth's atmosphere. However, in the balloon experiments, the photons emitted from the airborne sources get partially attenuated as they only travel through a fraction of the Earth's atmosphere.

AstroCal, however, takes these experiments to the next level by utilizing a nanosatellite as the payload carrier. While balloons can usually reach maximum altitudes of 10 - 30 km (i.e. upper troposphere to mid stratosphere), spacecraft in Low Earth Orbit (LEO) go as far as 500 - 2000 km from the surface of the Earth (although orbits between 600 to 800 km are preferred LEO orbits since there are more launch services available for this range). The high altitude of spacecraft allows for precise calibration of ground telescopes, since 99.99% of Earth's atmosphere is below the *Karman line* at 100 km altitude.

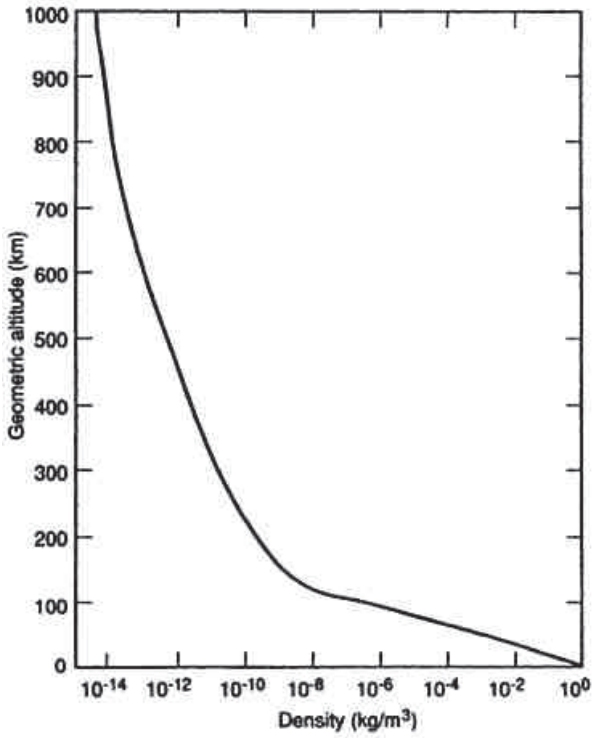


Figure 1.1: Atmospheric mass density as a function of altitude [2].

### 1.1.1 Experiment Background

Dark energy is an enigmatic form of energy that is causing the universe to expand at an accelerated rate, which makes up 75% of what the entire universe is composed of. In order to determine the amount and properties of dark energy in the universe, the light arriving

from supernovae are carefully studied with the goal to quantify how much redshift occurs to the light as it travels through the universe, from supernovae to the ground telescopes, due to the gravitational forces exerted by dark energy. On the other hand, in order to study the light, it is required to first calibrate ground telescopes against atmospheric and optical losses which is traditionally achieved through the observation of a series of starts that have had their light output in various bands of photometric system measured very carefully [9] (known as "standard stars"). However, a systematic limitation imposed on all traditional optical calibrations is the precision of these measurements and the fact that all stars have some level of variability in their output. An alternative approach to overcome this limitation is the use of man-made visible sources of light with luminous output measurable to a precision of up to 100 times better [10] than stellar sources, allowing for vast reduction of astronomical and cosmological uncertainties caused by atmospheric and instrumental extinction.

Another series of observations are made to discover the polarization patterns in the cosmic microwave background which encode a vast amount of other information (beyond dark energy) about the early universe. The interpretation of these measurements is essentially dependent upon an accurate calibration of sensitivity of the polarized instrument. No well-calibrated, polarized, celestial microwave sources have been developed thus far, making this deficit the limiting factor in the measurement and analysis of polarized microwave sky in the future generation of microwave telescopes. In addition, current calibration solutions in the microwave spectrum rely on relatively nearby ground-based sources, requiring refocusing and special low-sensitivity detectors to handle the near-field source and additional atmospheric loading.

The AstroCal mission, however, offers a practical solution to greatly reduce the systematic uncertainty explained above. On one hand, as part of the optical payload aboard the AstroCal spacecraft, there will be a source of light which will be used for accurate characterization of the attenuation of light due to the Earth's atmosphere as well as losses due to the optics in telescopes. On the other hand, there will be an one-of-a-kind accurately calibrated microwave source carried by AstroCal spacecraft that will be used to calibrate ground telescopes in the microwave region.

### 1.1.2 Calibration Method

The AstroCal spacecraft carries several payload instruments which can be categorized in two groups: *a*) optical payload; and *b*) microwave payload.

The optical payload refers to all instruments on board AstroCal spacecraft that are

intended for calibration of ground telescope in the visible light and near infrared spectrum (i.e., wavelengths ranging from 400 nm to about 800 nm). The microwave payload, on the other hand, is responsible for producing electromagnetic waves in the microwave region and consequently will be used to calibrate ground instruments in microwave region. A summary of the AstroCal payload instruments and their functionalities is presented in Table 1.1. A more detailed description of payload instruments is presented in Section 1.4.

Table 1.1: AstroCal payload instruments.

| **Spectrum** | **Component** | **Functionality** |
|---|---|---|
| Visible | MCL module | Produces light at four different wavelengths, as specified by the principal investigator at UVic ($\lambda_1 = 445$ nm, $\lambda_2 = 600$ nm, $\lambda_3 = 650$ nm, and $\lambda_4 = 750$ nm). |
| | Optical path | Transmits light from the MCL module to the integrating sphere. |
| | Integrating sphere | Scatters and diffuses light produced by the MCL module. |
| Microwave | Microwave source | Radiates electromagnetic waves in the microwave spectrum. |

Regardless of the type of payload (i.e., optical or microwave), the calibration is done in the following sequential steps:

1. On the spacecraft:

   *i.* The source of electromagnetic wave starts to operate.

   *ii.* The aperture of the payload is pointed toward a ground station telescope.

   *iii.* The radiance of the electromagnetic wave is measured inside the integrating sphere (carried on spacecraft) (denoted by $M_1$).

2. In the Earth's Atmosphere:

   *i.* The electromagnetic waves traveling to the ground telescope become attenuated due to absorption and scattering of photons by the Earth's atmosphere.

3. On the ground:

   *i.* The electromagnetic waves are further attenuated as they travel through the optics inside the telescope (such as filters, mirrors, lenses, etc).

*ii.* At last, the radiance of the arriving electromagnetic wave is measured (denoted by $M_2$).

*iii.* The values of $M_1$ and $M_2$ are compared and their differences are analyzed for characterization of losses due to the Earth's atmosphere and the optical instruments.

Fig. 1.2 shows a graphical interpretation of the AstroCal mission concept.

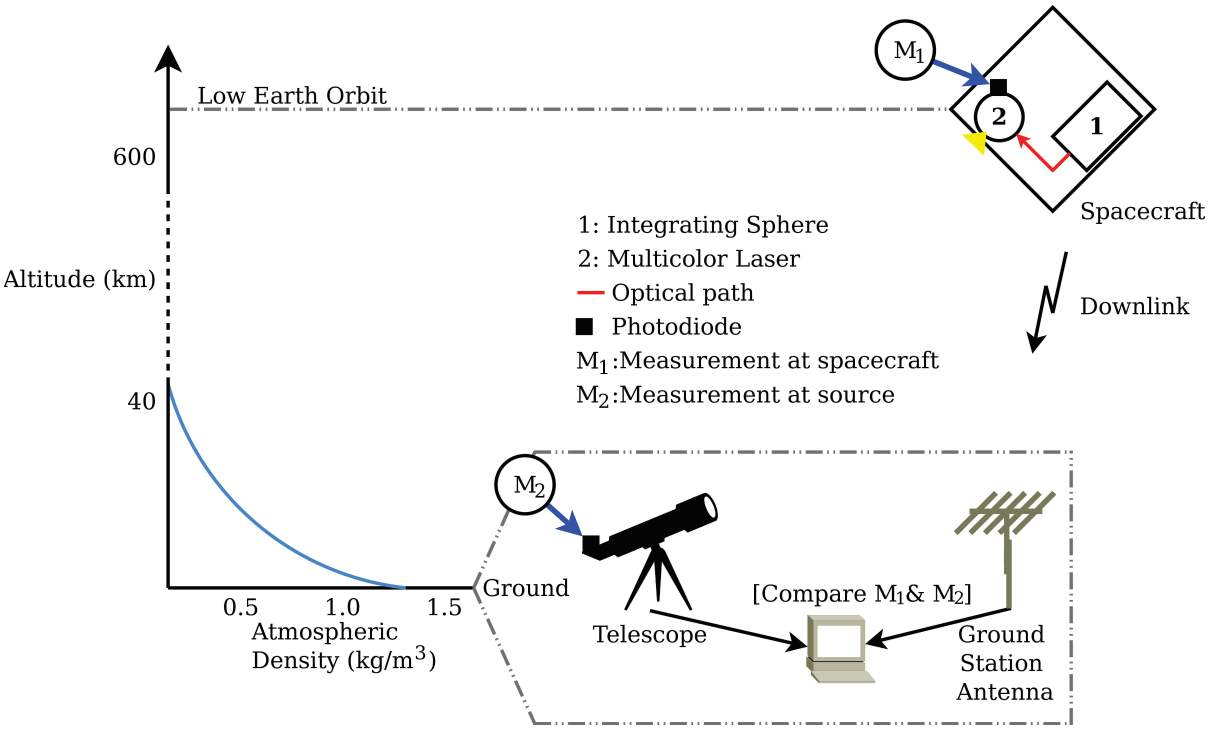


Figure 1.2: Author's depiction of AstroCal Mission Concept.

### 1.1.3 Generic Nanosatellite Bus

As of May 8, 2015, the GNB platform has about 178 months of operations heritage in space and has been used in nine different missions (AISSat-1 & 2, CanX-4 & 5, and five spacecraft in the BRITE[1] constellation), making it the spacecraft bus with the longest space heritage at SFL. The motivation for the design of GNB dates back to when the BRITE constellation program, as well as the CanX-4 & -5 mission initially started. In order to reduce the recurring cost, the design and development of a generic bus, which meets the requirements of both programs, was proposed. As it turned out, both missions

[1]BRITE stands for Bright Target Explorer

had similar power, payload volume, and data processing requirements [3], which is fulfilled by the GNB form factor.

The overall layout of the GNB is a cube measuring 20 cm to a side. Structurally, the bus is made up of six panels and two trays, which increase the rigidity of the bus and provide a compartment for computers and flight avionics. In between the two trays, there exists a dedicated payload volume with dimensions of 17 cm $\times$ 13 cm $\times$ 8 cm. An exploded view of the GNB form factor is shown in Fig. 1.3.

The standard[2] architecture of GNB can be divided into seven subsystems: structures, thermal control, power, Command and Data Handling (CDH) , communication, attitude determination and control, and payload. A brief description of each subsystem is presented below.

#### 1.1.3.1 Structural Subsystem

As mentioned previously, the structural design of the GNB is a dual tray design with a standard payload bay in between two trays, encapsulated by six panels. The two trays combined with the payload support structure are the main source of structural rigidity against vibration and shock loads during the launch. The modular design of the GNB allows for easy access to the payload bay and the instruments inside the two trays by simply removing one of the panels, avoiding the need to take the spacecraft fully apart. Finally, there are two launch rails incorporated directly into the trays, which are used to guide the spacecraft as it is sliding out of the XPOD deployment system.

#### 1.1.3.2 Thermal Control Subsystem

Thermal control subsystem consists of hardware that is used to control the temperature of all spacecraft components. On GNB, thermal control is achieved mostly by passive methods (using thermal tapes attached to the exterior of the panels, and regulating heat conduction within the spacecraft by utilizing appropriate mounting strategies for components). There is, however, a battery heater included to keep the batteries sufficiently warm to avoid any damages during charging.

#### 1.1.3.3 Power Subsystem

The power subsystem includes all equipments that are used to generate and distribute electrical power to the spacecraft, which includes solar cells, batteries, power converters,

[2]The word "standard" is used here to distinguish between the subsystems that appear on all Generic Nanosatellite Buses and those that are mission specific, such as the propulsion subsystem on CanX-4 & 5 spacecraft

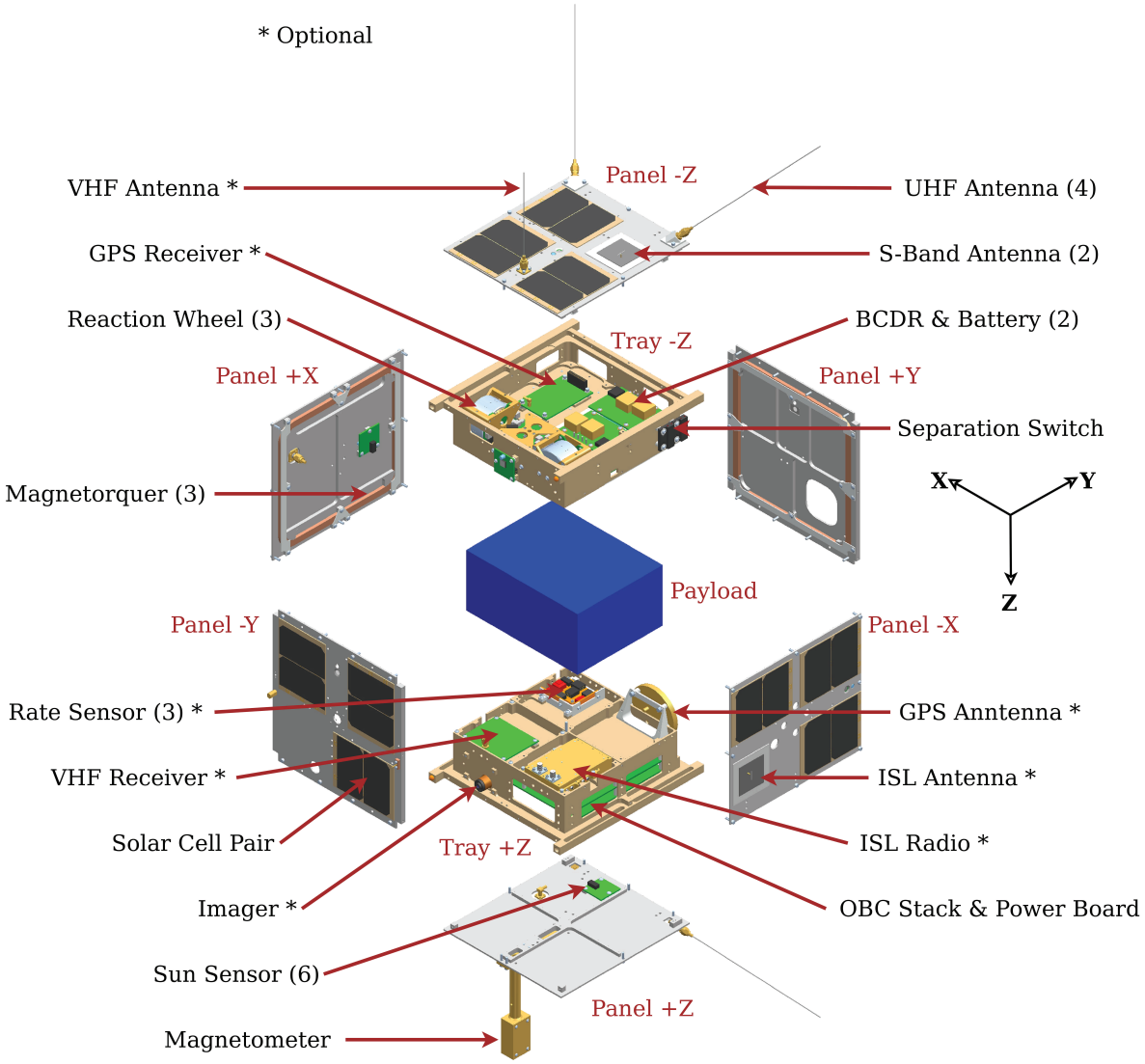


Figure 1.3: An exploded view of GNB platform (replicated from [3]).

wiring harnesses, battery-charge-discharge-regulators (BCDR), among others. In addition, there are two magnetic reed switches (also known as "separation switches"). In the presence of a magnetic field, these switches are closed. On GNB (and other platforms), these switches are used to keep the spacecraft off while it is in the XPOD [3] separation system. Upon separation from XPOD and in the absence of its powerful magnetic field, the reed switches revert to their nominal open position, allowing power supply to the power board and turning the spacecraft on.

[3]XPOD is the separation system that is developed by SFL, and is used to separate nanosatellites from any launch vehicle. They are available in various different standard models: XPOD Single, XPOD Duo, XPOD Triple, etc.

#### 1.1.3.4 Command and Data Handling Subsystem

Also known as the computer subsystem, the CDH subsystem of GNB includes several components such as two On-board Computer (OBC)s: a Housekeeping Computer (HKC), and an Attitude Determination and Control Computer (ADCC). There is also the possibility that a third OBC be included to control and command payload instruments exclusively, which is referred to as the Payload On-board Computer (POBC).

The CDH subsystem is also responsible for receiving commands from the communication subsystem, and distributing the commands to appropriate spacecraft subsystems after validation and decoding via the use of the software codes residing on the OBCs.

#### 1.1.3.5 Communication

The communication subsystem of GNB is composed of two different radio modules operating at different wavelengths, as described below:

1. S-band radio, which includes a transmitter and two patch antennas (mounted on the exterior of two opposite panels in order to maximize the coverage), which is used to transmit (or *downlink*) telemetry data from spacecraft to the ground station.

2. UHF radio, which includes a receiver and four unidirectional antennas (mounted on four adjacent vertices, almost extending away from the bus, along the space diagonal of GNB form factor), which is used to receive signals that are transmitted from the ground station to the spacecraft (known as "uplink").

Additionally, GNB spacecraft may also be equipped with an intersatellite link (ISL) radio for data exchange between two spacecraft (perhaps that are flying in formation, as in CanX-4 & 5), and may be equipped with a VHF-beacon radio, which provides a simple means to acquire spacecraft health and tracking [11].

#### 1.1.3.6 Attitude Determination and Control Subsystem

As the name suggest, the Attitude Determination and Control Subsystem (ADCS) is responsible for *a*) attitude determination using the on-board attitude sensors; and *b*) attitude control using the attitude actuators.

The attitude determination of the spacecraft is achieved by six sun sensors, a three-axis magnetometer that is mounted on a pre-deployed structure extending away from the spacecraft bus to minimize the magnetic noise induced by the on-board electronics, and an optional three-axis rate sensor that may be used if the pointing requirements indicate

so. Another optional attitude determination sensor is a star tracker, which is used for fine pointing determination.

The attitude control of the spacecraft is achieved by three reaction wheels that provide fine adjustment of spacecraft attitude, as well as three magnetic torquers (also known as "magnetorquers") on printed circuit board (PCB) that are mounted on the interior of the panels, and are used for coarse attitude adjustments.

#### 1.1.3.7 Payload Subsystem

The payload subsystem occupies a volume of 13 cm × 17 cm × 8 cm located in between the two trays (see Fig. 1.3). This volume is strictly allocated to the payload instruments and hence any non-payload components are not allowed in this volume. Similarly, no components of the payload can extend beyond the allocated payload volume. Further, the payload is always supported by the trays introduced in Section 1.1.3.1, and impose no direct bearing on the spacecraft panels. In addition, there may be other supportive structures inside the payload volume, which not only hold the payload instruments in place, but also improve the overall rigidity of the spacecraft by providing solid support to the trays. It is expected that the payload as a whole weighs less than a kilogram and be able to withstand vibrations and shock loads that are induced by the launch vehicle (characteristics of these loads depend on the type of the launch vehicle that is used for a specific mission). lastly, thermal control of the payload subsystem is usually achieved via passive means, such as thermal tapes and body-mount radiators.

## 1.2 AstroCal Mission Study Deliverables

As mentioned previously, the objective of the AstroCal mission study is to demonstrate the feasibility of a high-precision astronomical calibration mission using a nanosatellite. Aside from the activities that are focused on the development of the spacecraft bus for the mission, in the AstroCal mission study the author has also been in charge of the conceptualization and design of the payload instruments under the supervision of the principal investigator at UVic. The design of the payload instruments is detailed enough that, upon funding approvals and commencement of the next phases of the mission, they can be used as the framework for development of the actual modules, hence significantly shortening the development time.

By the end of the AstroCal mission study, SFL was expected to deliver the following:

- A fully grown spacecraft solid model.

- A detailed design for each instrument listed in Table 1.1.
- Results of the analyses that are performed to prove the feasibility of AstroCal mission carried out by a nanosatellite.

One of the most important aspects of such mission studies at SFL is to adapt an *existing* spacecraft bus to the mission. This approach provides many logistical advantages, some of which are listed below:

- It minimizes the lead time that is required to design and develop a spacecraft from the ground up.
- Most spacecraft components are available in stock, eliminating the long wait-time required for their fabrications.
- Higher reliability and longer space heritage that these instruments have acquired through previous missions, which improves the chances of a successful mission.
- While traditional space missions are strictly top-down and requirement-driven, this approach fuses the bottom-up capability-driven , and the combination greatly reduces the overhead and schedule costs of systems development.

## 1.3 Adaptation of GNB Platform to AstroCal Mission

The AstroCal spacecraft is based on the GNB platform, which has a payload volume with a length of 17 cm, a width of 14 cm, and a height of 8 cm. During the AstroCal spacecraft development and as the payload design was maturing, it was realized that the standard payload volume of GNB is insufficient (in width) to accommodate the AstroCal payload. Hence, it was proposed to increase the width of the allowable payload volume by 1 cm while maintaining the overall payload mass to below 1 kg. Before committing the payload volume increase, however, it was required to investigate whether such an expansion would interfere with any other parts of the bus, especially the wiring harnesses that run between the two trays. To do so, the solid model from the previous missions that had used GNB form factor as well as the AstroCal spacecraft solid model were scrutinized. Since the GNB bus is based on a *modular* design, in the end it was concluded that by re-routing some of the wiring harnesses, the 1-cm expansion will not introduce any serious problem with spacecraft development. Hence, the payload volume allocated to AstroCal spacecraft is 1 cm wider on AstroCal spacecraft (see Fig. 1.4).

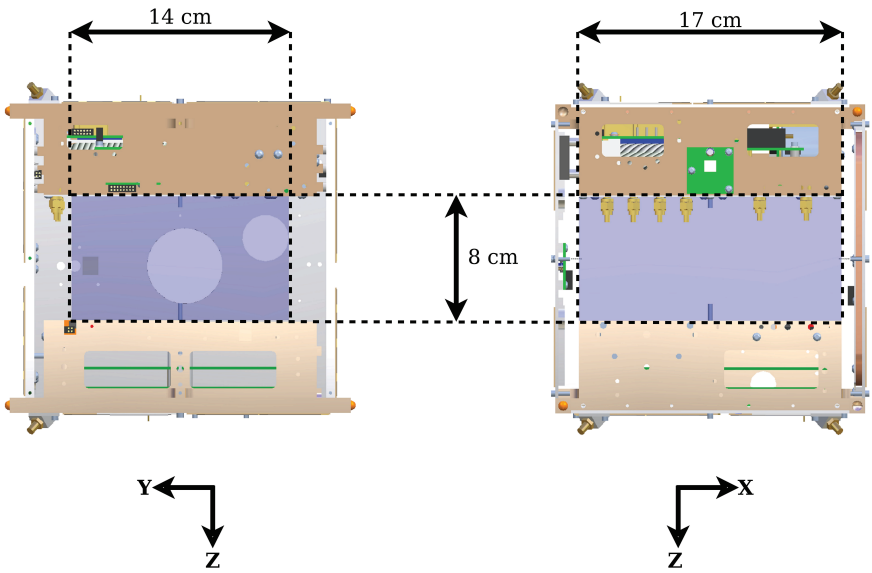


Figure 1.4: Modified GNB payload bay for the AstroCal mission study.

In order to support the payload of AstroCal spacecraft, two truss structures (called "-X truss" and "main truss") are designed (see Fig. 1.5). As the name suggest, the -X truss is located on the -X side of the spacecraft and connects to the each tray via three mounting points (i.e. in total six mounting points). On the other hand, the main truss is located in between the trays and serves as a multi-purpose payload structure: it provides mounting points for the payload instruments, as well as additional support to the overall structure of GNB by connecting to each tray at two points (two of which are located on the +X side, and the other two in the middle of the payload bay). Combined together, the truss structures provide additional support against any torsional forces about all three axes of the spacecraft.

Another aspect of the adaptation of the standard GNB platform to the AstroCal mission is the placement of the solar cell coupons on each panel of the spacecraft. This is primarily achieved by determining the available surface area on each panel, and further by the power requirements that are imposed by spacecraft and its payload. The available surface area is determined after all cutouts are made to the panels in order to create room for the apertures of the instruments, as well as holes for routing solar cells' wires to their respective boards inside the spacecraft, and leaving the appropriate amount of surface area required for the thermal control of the spacecraft. As so, the AstroCal spacecraft has four panels (i.e., +Y, −Y, +Z, and −Z panels ), each of which having eight coupons, and two panels (i.e., +X and −X) with four coupons attached on them. On the −X panel,

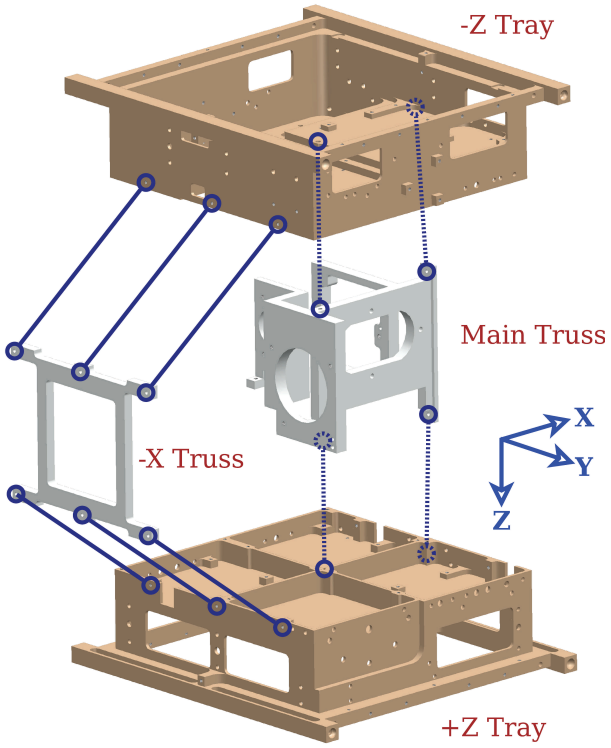


Figure 1.5: Connection points of the truss structures to the trays.

there are two relatively large circular cutouts: one for the integrating sphere output port which is 4.9 cm in diameter, and one for the microwave source, which is 3.0 cm in diameter. Similarly, on the +X panel, there are two large cutouts: a rectangular cutout for the payload radiator with dimensions of 5.8 cm × 5.4 cm, and a circular cutout for sthe aperture of the tar tracker which is 2.0 cm in diameter (see Fig. 1.6). As a result of these modifications, there is enough surface area for 40 solar cell coupons to be attached on the exterior of the AstroCal bus.

## 1.4 Spacecraft Payload Development

The optical payload aboard AstroCal spacecraft consists three main instruments:

1. a multicolor laser (MCL) module,
2. an optical path unit, and
3. an integrating sphere.

The microwave payload, on the other hand, consists of a single microwave source unit. In addition, there is a star tracker (as part of the ADCS) that is directly mounted to the

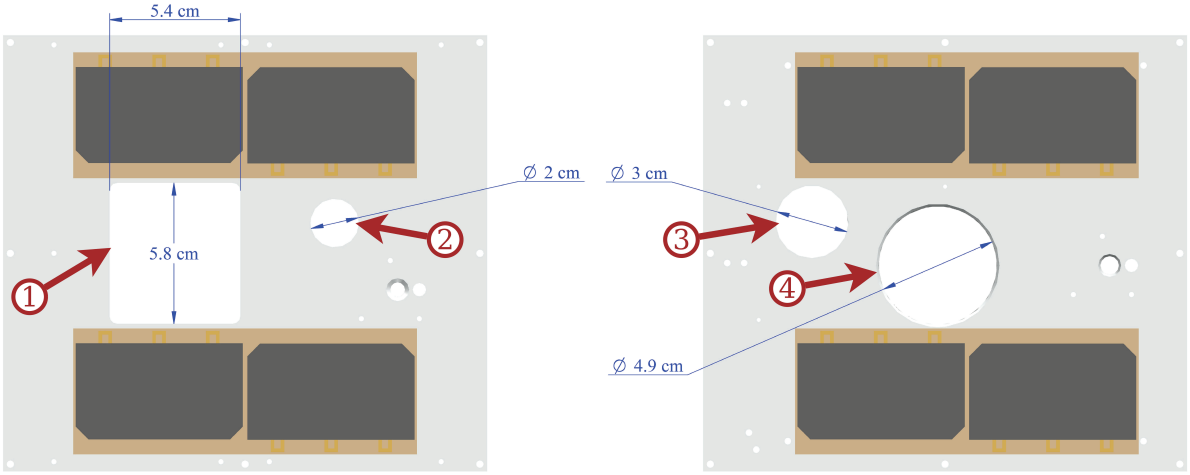


1: Payload radiator, 2: Star tracker, 3: Microwave source, 4: Integrating sphere

Figure 1.6: Cutouts on the +X panel (left) and the −X panel (right) of the AstroCal spacecraft.

main truss. Rigidly connecting the star tracker to the main truss ensures that transient misalignments between the payload and the ADCS caused by thermal expansion are minimized.

Fig. 1.7 shows the instruments that are included in the payload volume. In what follows, a detailed description of each instrument will be provided.

### 1.4.1 Multicolor Laser Module

The MCL module is an optical instrument that is designed in-house, and is capable of producing light with four different colors, corresponding to the wavelengths listed in Table 1.1. Traditional multicolor laser systems are comprised of several single-color laser modules, each capable of producing light with a distinct color. As a result, they occupy large volumes and are generally too heavy to be considered for nanosatellite space missions. Another drawback of the traditional multicolor laser systems is that the output of each laser module in the system is guided to the final destination through optical fibers. However for AstroCal, one of the main requirements is that in the design of the MCL module, no optical fibers shall be used. This is due to the fact that optical fibers are lossy means of transmission. Their performance further degrades when they are under vibration and temperatures swings, both of which are common phenomena when carried on a spacecraft.

The MCL module designed for the AstroCal mission is an optical instrument with dimensions of 9.6 cm × 5.6 cm × 4.1 cm and a mass of 399.6 g, which can be easily

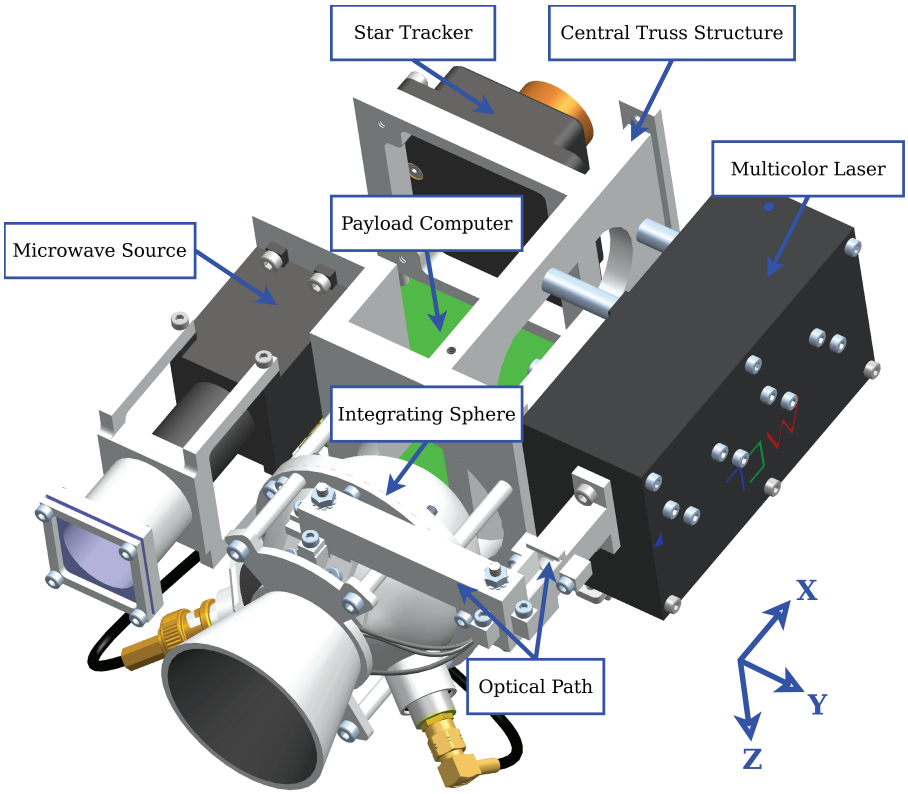


Figure 1.7: AstroCal payload instruments.

incorporated in the AstroCal payload by connecting to the main truss structure through four mounting points. Further, it provides a 9-pin serial port for connection to the POBC. The module consists of smaller units (known as "wedge unit") that are explained in Section 1.4.1.1.

#### 1.4.1.1 Wedge Unit

Inside the MCL module's housing, there are four wedge-shaped units (referred to as "wedge unit" henceforth), each of which is responsible for producing light with a specific color. In each wedge unit, a laser diode is the source of light. Dichroic mirrors, on the other hand, are responsible for guiding the light toward the exit port of the MCL module. They are mounted on the wedge-shaped central structure via a spring-loaded mechanism. As a result of the shape of the central structure, there is a 45° angle between the dichroic mirror's surface and the axis along which laser beams are emitted from a laser diode.

Dichroic mirrors have combined mirror-like and filter-like characteristics: they are capable of reflecting light within certain wavelength range, while transmitting others. There are two distinct types of dichroic mirrors: *a*) shortpass; and *b*) longpass. A short-

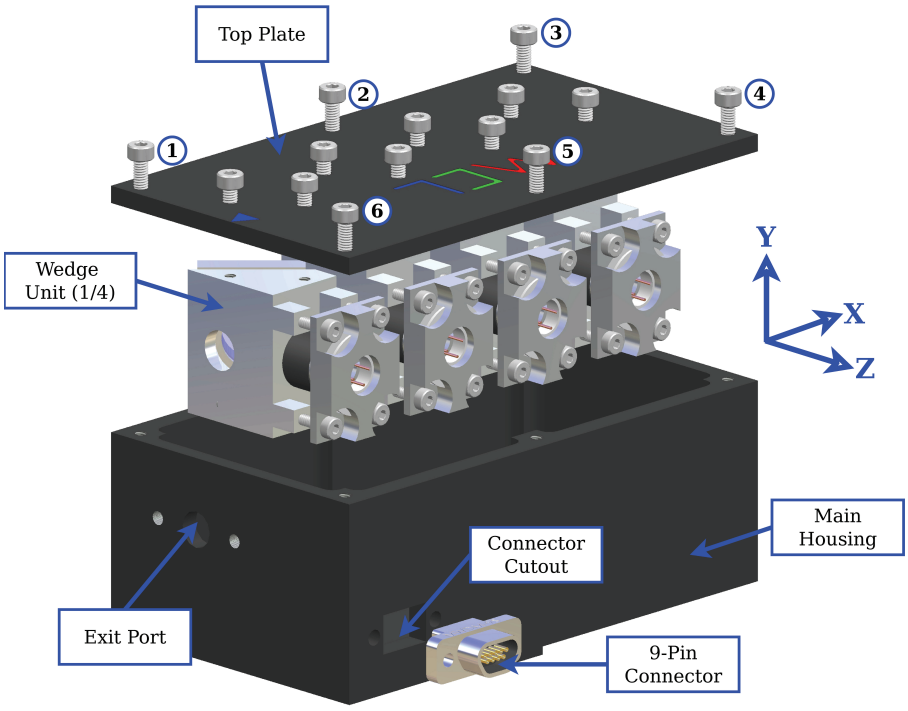


Figure 1.8: An exploded view of the multicolor laser. The top plate, which secures the wedge units, gets mounted to the main housing via screws 1-6.

pass dichroic mirror allows light with wavelengths shorter than the cut-off wavelength pass through while reflecting longer wavelengths. In contrast, a longpass dichroic mirror allows light with wavelengths longer than the cut-on wavelength pass through while reflecting shorter wavelengths. The dichroic mirrors that are used in the MCL module are 1.25 cm in diameter and 0.01 cm thick, and are supplied by Edmund Optics® (EO). Table 1.2 provides a list of the selected dichroic mirrors, as well as their wavelength ranges. Two sample transmission and reflection diagrams belonging to DM1 and DM2 from Table 1.2 are provided in Appendix A.2.

The sources of light in the MCL module are four standard 9 mm laser diodes with output wavelengths as listed in Table. 1.1. Each wedge unit includes a laser diode whose output beam goes through a collimating lens before arriving to the dichroic mirror. The diodes selected for this study are supplied by RPMC Lasers Inc.

#### 1.4.1.2 Principle of Operation

The principle of operation of MCL is illustrated in Fig. 1.10. In each wedge unit, a laser diode emits a laser beam which arrives at the dichroic mirror included in that wedge. The

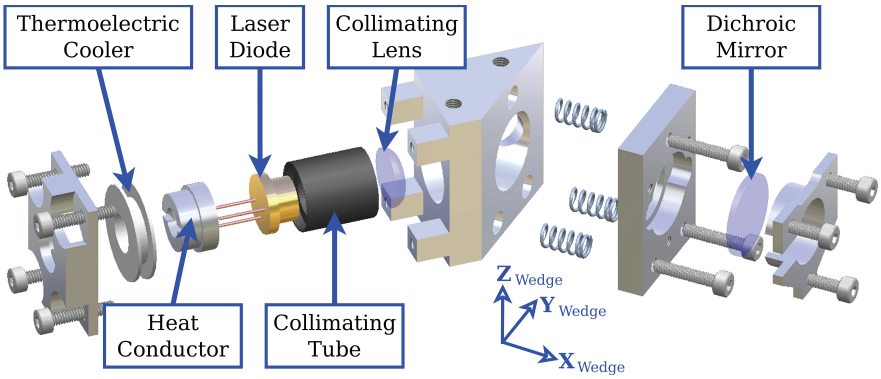


Figure 1.9: An exploded view of a wedge unit in the multicolor laser module.

Table 1.2: Selected dichroic mirrors for the multicolor laser module in the AstroCal mission study.

| Name | EO Stock No. | cut-off/-on Wavelength (nm) | $\lambda_{Tx}$ † (nm) | $\lambda_{Rx}$ ‡ (nm) | Type |
|---|---|---|---|---|---|
| DM1 | 69-866 | 500 | 520 - 1600 | 350 - 480 | Longpass |
| DM2 | 69-180 | 600 | 400 - 580 | 625 - 795 | Shortpass |
| DM3 | 69-181 | 650 | 400 - 630 | 675 - 850 | Shortpass |
| DM4 | 69-183 | 750 | 400 - 725 | 800 - 990 | Shortpass |

† Transmission wavelength; ‡ Reflection wavelength.

dichroic mirror, which makes a 45-degree angle with the beam direction, reflects the laser beam toward the output port of the MCL (i.e., the beam changes direction by 90°). The beam travels through the next dichroic mirrors and passes through them without any further reflections. The laser diodes are selected and positioned such that the wavelength of their output is within the transmission wavelength of the dichroic mirrors in the next wedge units.

As shown in Fig. 1.10, the laser beam produced by LD1 will have a wavelength of 445 nm, which is within the reflection wavelength range of DM1 (i.e., 350-480 nm), and therefore will be reflected by DM1. However, the DM2 has been selected such that it allows the output of LD1 to pass through, since the wavelength of the output of LD1 (i.e. 445 nm) is within the transmission wavelength range of DM2 (i.e. 400-580 nm). This principle applies to all other laser diode-dichroic mirror combinations that are incorporated in the MCL module. A summary of the principle of operation of the MCL module is presented in Table. 1.4.

One important advantage of this method is the elimination of any optical fibers and

Table 1.3: Selected laser diodes for the multicolor laser module in the AstroCal mission study.

| Name | RPMC Part No. | Wavelength (nm) | Output Power (mW) | Operating Temperature (°) |
|---|---|---|---|---|
| LD1 | LDX-310-445 | 445 | 1,000 | 25 |
| LD2 | LDX-2410-630 | 630 | 400 | 15 |
| LD3 | LDX-3230-680 | 680 | 1,400 | 25 |
| LD4 | LDX-3765-808 | 808 | 7,000 | 20 |

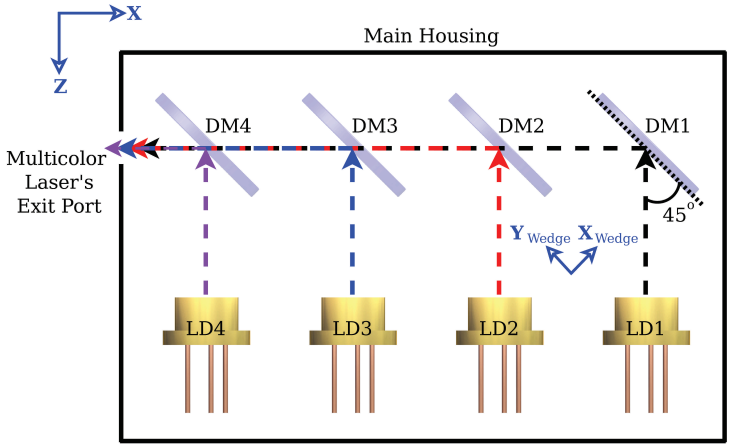


Figure 1.10: Top view of inside of the multicolor laser (simplified model). Dashed arrows represent the light emitted by each laser diode. DM: Dichoric mirror; LD: Laser diode.

splitters that would otherwise be needed to guide the outputs of the laser diodes along the axis of the MCL module's output port.

#### 1.4.1.3 Assembly Procedure

In the design of the MCL module, a great deal of attention has been paid to the order in which the module comes together. This is due to the fact that the module is composed of several small components (optical and structural) that have to be positioned at specific locations in specific orders. As a result, the MCL module is made up of four wedge unit sub-assemblies which can be put together independent of each other, as well as the housing structures (a top plate and a hollow rectangular prism which is missing a base and is called "main housing"). Once the wedge unit sub-assemblies are created, the MCL module can be formed simply by mounting each of the wedge units to the top plate. Finally, the top plate which now has four wedge units assembled to it can be secured

Table 1.4: Principle of operation of the MCL module. LD: laser diode; DM: dichroic mirror.

| | | **Dichroic Mirrors** | | | |
|---|---|---|---|---|---|
| | | DM1 | DM2 | DM3 | DM4 |
| **Laser Diodes** | LD1 | Reflection | Transmission | Transmission | Transmission |
| | LD2 | - | Reflection | Transmission | Transmission |
| | LD3 | - | - | Reflection | Transmission |
| | LD4 | - | - | - | Reflection |

to the main housing structures via six screws. A more detailed assembly procedure is provided below.

1. Dichroic mirror sub-assembly: assemble the dichroic mirror sub-assemblies.
2. Laser diode sub-assembly: assemble the laser diode and the related components (i.e., collimating lens and tube, thermoelectric cooler, etc) to the wedge-shaped central structure.
3. Wedge unit: mount the dichroic sub-assembly to the laser diode sub-assembly . Repeat steps 1-3 three more times.
4. Route wires from the laser diodes in each wedge unit (through the connector cutout) to the serial connector.
5. Top plate sub-assembly: mount each wedge unit to the top plate.
6. Multicolor laser module: fasten the top plate sub-assembly as well as the serial connector to the main housing.

Fig. 1.11 illustrates the order of assembly of the MCL module (wire connections not shown).

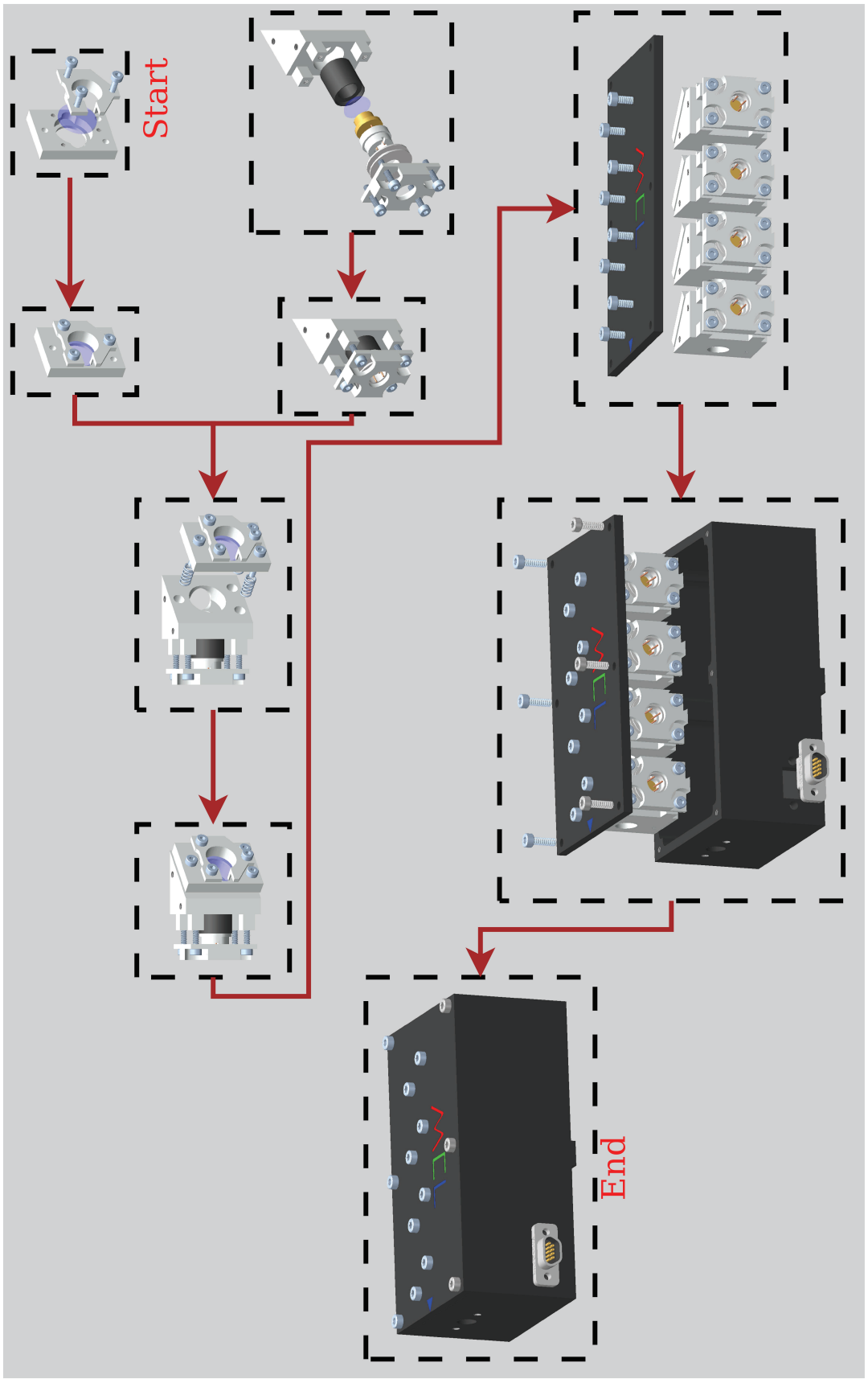


Figure 1.11: Order of assembly of the multicolor laser module .

### 1.4.2 Integrating Sphere

An integrating sphere is an optical component consisting of a hollow spherical cavity with its interior covered with a diffuse white reflective coating, with small holes for entrance and exit ports. Its relevant property is a uniform scattering or diffusing effect. Light rays incident on any point on the inner surface are, by multiple scattering reflections, distributed equally to all other points. The effects of the original direction of light are minimized. An integrating sphere may be thought of as a diffuser which preserves power but destroys spatial information. It is typically used with some light source and a detector for optical power measurement.

In the AstroCal mission study, an integrating sphere with a diameter of about 2 inches have been selected mainly due to spatial constraints imposed by the available payload volume on GNB platform. Two photodiodes have been also selected by the principle investigator to increase the accuracy of in-flight measurements (see Fig. A.1 in Appendix A.1).

Around the output port of the integrating sphere, a set of six light emitting diodes (LED) is mounted. The rationale behind the inclusion of these LEDs is as follows: *a*) they are additional available light sources, of a different type than the laser diodes; and *b*) they are used for in-flight calibration of the photodiodes.

### 1.4.3 Optical Path

As mentioned previously, one of the main deriving payload requirements for AstroCal mission study is that no optical fibers shall be used in the design of the MCL or any other payload instrument. As an alternative solution, a system of multiple mirrors is selected which is capable of guiding the light from the output of the MCL toward the entrance port of the integrating sphere. Similar to optical fibers, mirrors attenuate light at each reflection. Therefore, reducing the number of mirrors leads to attenuation reduction.

Given the arrangement of of the payload instrument on AstroCal's spacecraft, a minimum of two mirrors are required. However by adding one more mirror to the design of the optical path, the geometry and shape of the optical path becomes much more simpler.

The mirrors that have been considered in AstroCal mission study are mounted to a metallic post at a 45° angle. The posts have threaded ends, which allow for mounting the mirror to the optical path structure as well as adjusting their heights.

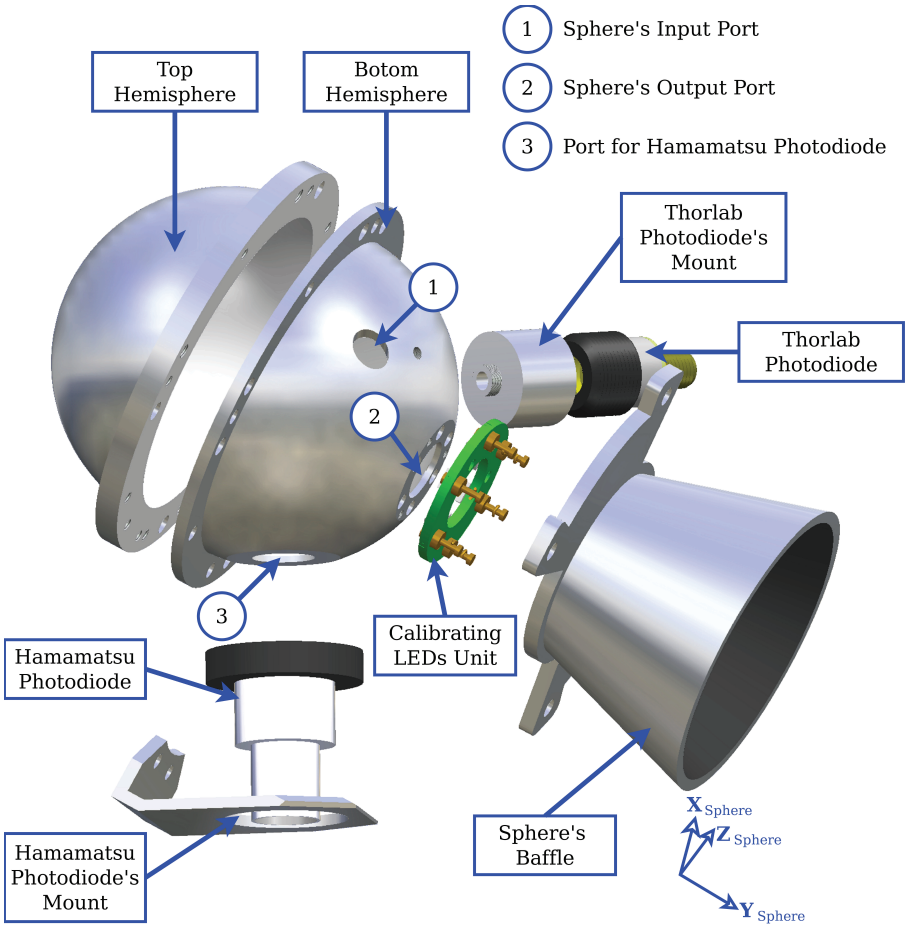


Figure 1.12: An exploded view of the integrating sphere (screws and standoffs not shown). The laser beam produced by MCL enters the sphere via the sphere's input port and exits it via the output port (port numbers 1 and 2, respectively).

#### 1.4.3.1 Analysis of Optics Misalignments

As the laser beam travels from its source (i.e, a laser diode) to the final destination (i.e., integrating sphere), it interacts with several optical media. Firstly, it passes through the dichroic mirrors inside the multicolor laser. Secondly, it is reflected off the surface of the small mirrors. These interactions cause divergence of the laser beam from its optimal path (the path on which the beam would have traveled if there were no non-idealities in the optical interfaces, such as misalignments, etc). Therfore it is necessary to analyze the path of the beam to determine whether the magnitude of the linear divergence becomes so large that it prevents the beam from entering the integrating sphere.

The purpose of this analysis is to quantify the amount of divergence that is caused by each of the optical media due to two sources of error:

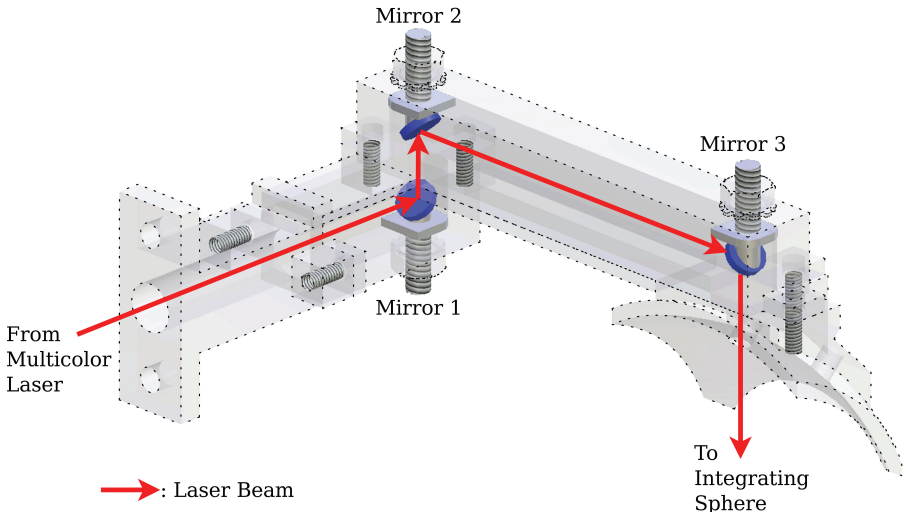


Figure 1.13: The see-through model of the optical path (screws not shown). Inside the optical path, light is reflected by three mirrors before entering the integrating sphere.

1. misalignment of the dichroic mirrors in the multicolor laser module.

2. misalignment of the small mirrors in the optical path.

Not included in this analysis are the other sources of error such as non-ideal properties of material of the optics that require an in-depth knowledge of materials and physics of optics.

As mentioned before, the dichroic mirror is mounted to the wedge-shaped central part via a spring-loaded structure, which allows for a precise adjustment of the angle between the dichroic mirror's surface and the laser beam axis, achieved by tightening or loosening of each adjustment screws (see Fig. 1.14). On the other hand, the small mirrors inside the optical path have flanges which are responsible for alignment of the mirrors.

Three assumptions are made in order to perform the analysis:

- The adjustment screws used to calibrate the angle of the dichroic mirror surface with respect to the axis of the beam can only be rotated in 10-degree steps.

- The surface of the flanges in the small mirrors are machined with a tolerance of five thou (i.e., 0.005 inches).

- All divergences add up in one direction away from the optimal path direction (which would be the worst-case divergence analysis).

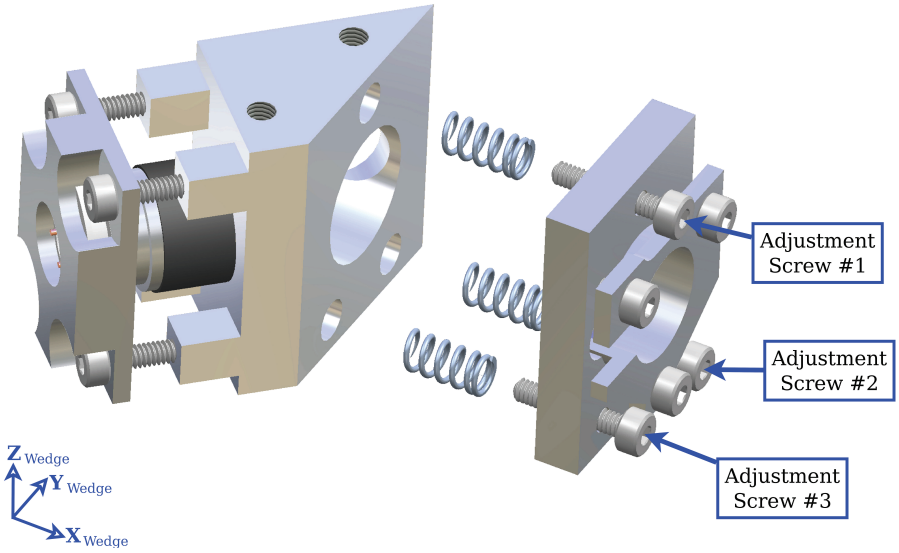


Figure 1.14: In each wedge unit, the orientation of dichroic mirror's surface can be adjusted using adjustment screws.

The first two assumptions allow to calculate the angular divergence that is caused to the the laser beam after interaction with each medium. The detailed discussions of divergence calculation due to each assumption is presented in Appendix A.3 and A.4. In summary, each dichroic mirror and each small mirror introduces an angular divergence of 0.033° and 1.2° to path of the laser beam respectively. the Since the beam emitted from laser diode in the wedge furthest from the output port of MCL module interacts with all optical media, and hence gets diverged the most, it will be the basis for the analysis. Fig. 1.15 shows the path of the beam emitted from LD1 to its destination, the integrating sphere.

The equation used to calculate the amount of linear divergence from the optimal path at point $k$ (denoted by $e_k$) given the angular divergence $\theta$ caused by each medium is as follows:

$$e_k = d_k \times \tan \sum_{i=1}^{k-1} \theta_i \tag{1.1}$$

where $d_k$ is the distance between the centers of two adjacent surfaces of media at points $k-1$ and $k$. The distances between the adjacent surface of the media are summarized in Table 1.5.

The total amount of linear divergence $E$ is the sum of all linear divergences from the

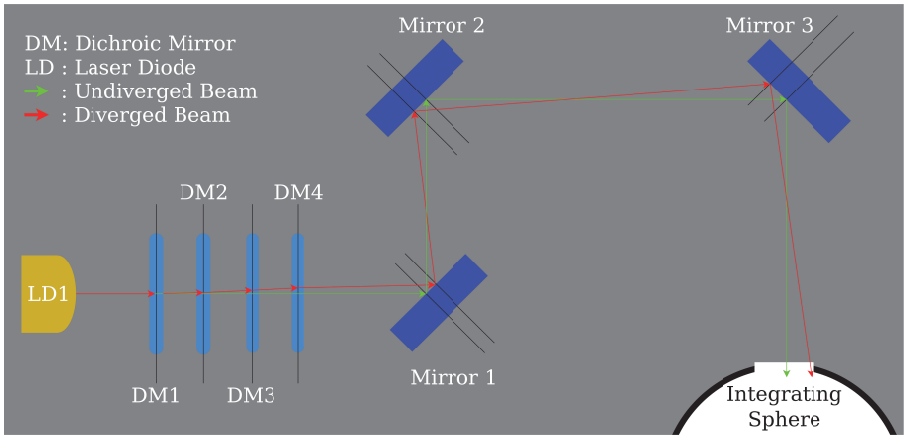


Figure 1.15: A 2 dimensional diagram showing the divergence of the laser beam emitted from laser diode 1 (LD1) after each transmission and reflection.

Table 1.5: Distances between the optical media in MCL and optical path

| **Variable** | **Desscription** | **Length (mm)** |
|---|---|---|
| $d_1$ | Distances between LD1 and DM1 | 15.58 |
| $d_2$ | Distances between DM1 and DM2 | 22.07 |
| $d_3$ | Distances between DM2 and DM3 | 22.07 |
| $d_4$ | Distances between DM3 and DM4 | 22.07 |
| $d_5$ | Distances between DM4 and M1 | 57.90 |
| $d_6$ | Distances between M1 and M2 | 8.64 |
| $d_7$ | Distances between M2 and M3 | 52.09 |
| $d_8$ | Distances between M3 and input port | 8.61 |

optimal path and can be calculated as follows:

$$E = \sum_{j=0}^{n} e_j. \tag{1.2}$$

Here, $n$ is the total number of optical media that the laser beam interacts with. For example, $n = 8$ for the laser beam emitted from LD1.

Fig. 1.16 shows the graph of linear divergence of the beam emitted from LD1 from the optimal path caused by interaction with the optical media as a function of distance from LD1.

There are two locations that are particularly important in this analysis. These two locations, i.e. the output port of the MCL module and the input port of the integrating

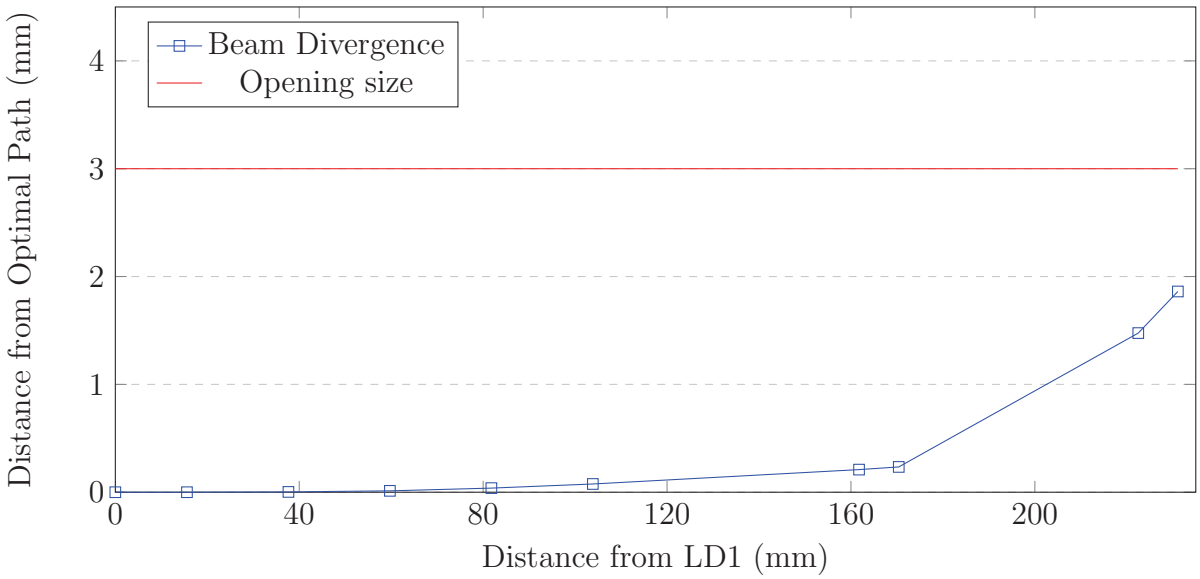


Figure 1.16: The linear divergence of beam emitted by LD1 from its optimal path as a function of the distance from LD1.

sphere, have the smallest opening sizes in the path of laser beam. The multicolor laser's output port is 6 mm in diameter (or 3 mm away from the optimal path since the optimal path passes through the center of the output port). Also, the integrating sphere's input port is 6 mm in diameter (or similarly, 3 mm away from the optimal path since the optimal path passes through the center of the integrating sphere's input port). As shown in Fig. 1.16, the laser beam stays clear from each of these two physical boundaries and in fact enters the integrating sphere.

### 1.4.4 Payload Architecture

As mentioned previously, one of the computers aboard the AstroCal spacecraft is the POBC which is responsible for commanding the payload instruments, as well as handling the data that is generated by the environmental sensors such as temperature sensors that monitor payload temperature at different locations. The OBC is mounted to the central truss structure toward the +Z side, inside the allocated payload bay. The inclusion of the payload computer inside the payload bay allows for reduction of the wiring harnesses' lengths that are required to connect each payload instrument to the POBC.

In the current architecture of the AstroCal's payload, the payload computer directly provides power to the payload instruments (see Fig. 1.17). The MCL module receives

power directly from the payload computer via a 9-pin serial connector (4 of which are used for power and the other four provide ground nodes). The calibration LEDs around the output port of the integrating sphere are mounted on a PCB. On the PCB, there are six Turret connectors to which six power lines are soldered. The photodiodes that are mounted to the integrating sphere are passive sensors and require only a data connection to the payload computer. Hamamatsu photodiode has a male BNC (Bayonet NeillConcelman) connection, therefore it requires a connector which has a female BNC connector on one end and a male MCX (micro coaxial) connector on the other end since the corresponding connection port on the payload computer is a female MCX connector. On the other hand, the Thorlab photodiode, has a male SMA (Subminiature Version A) connector on it, hence its connector requires a female SMA connector on one end and a female MCX connector on the other end. Finally, the microwave source requires a connecting wire which has angled female MCX connectors at both ends.

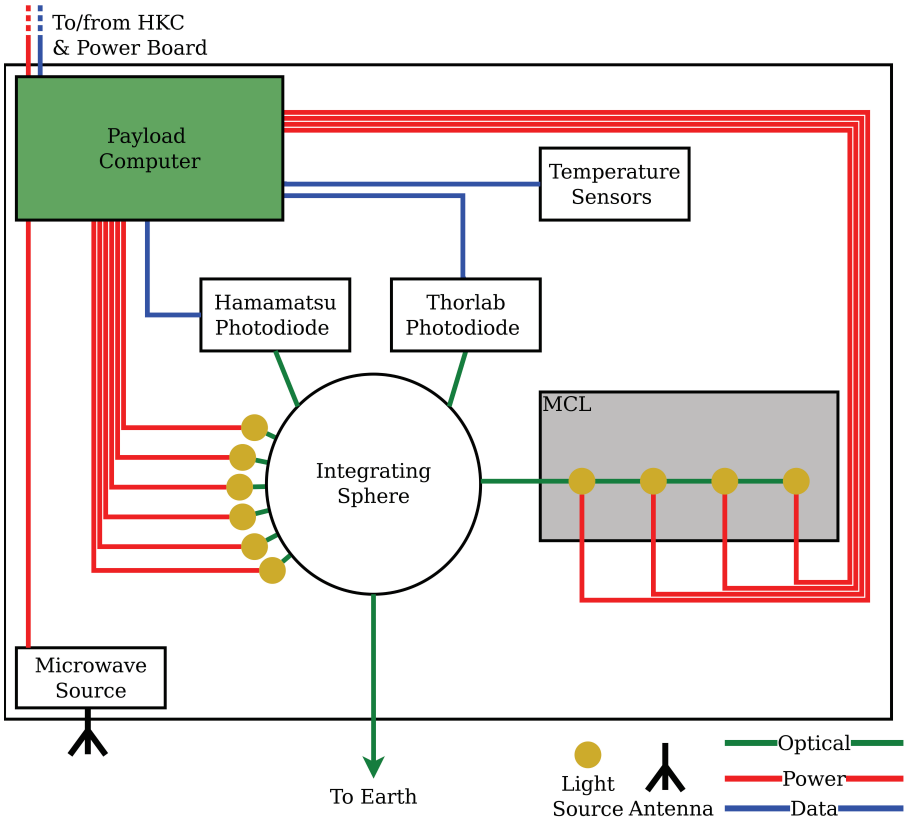


Figure 1.17: AstroCal payload architecture.

## 1.5 Spacecraft Mass Budget Analysis

The overall mass of any spacecraft that uses GNB platform cannot exceed 7.0 kg, according the specification sheet provided by SFL [12]. The 7-kg mass constraint includes the mass of every single component that is part of the spacecraft and remains with it after the spacecraft is detached from the launch vehicle. In order to keep track of the spacecraft mass throughout its development, and to avoid any unprecedented mass overage at the final stages of the mission development and close to the launch, every mission at SFL has a detailed mass budget document which is updated when component selections are made, spacecraft structural design is changed, or a better knowledge of the instruments' masses are gathered. In the end, a well-kept mass budget guaranties that spacecraft will in fact weigh less than the allowed total mass.

### 1.5.1 AstroCal System Level Mass Budget

A system level mass budget includes a list of all spacecraft subsystems and their estimated mass values, which is in turn deduced from a more detailed mass budget breakdown, called "subsystem level mass budget". The listed values in a system level mass budget include *contingency*, defined as the difference between the current best estimate and the maximum expected value [13]. Therefore, the higher the degree of uncertainty in the estimated mass of an instrument, the higher the contingency mass allocated to that instrument. In general, there are four different types of contingencies that are used in a mass budget, as described in Table 1.6.As the spacecraft design matures and mass of each piece of hardware becomes more certain, the contingency mass allocation is decreased.

Table 1.6: Contingency allocation to the spacecraft components based ounicertainties in mass estimations

| Code | Contingency | Description |
|---|---|---|
| E | 25% | Estimated mass |
| M1 | 5% | Measured from engineering or protoflight models |
| M2 | 0% | Measured from existing flight models |
| S | 0% | Specified in datasheets or interface control documents |

A summary of AstroCal spacecraft system level mass budget is presented in Table 1.7. The complete budget can be found in [14]).

At SFL, it is required that at the preliminary design review (PDR) stage of any spacecraft development (i.e., by the end of Phase-B), a 30% margin must be allocated in the mass budget [15]. The system level mass budget presented in Table 1.7 shows that

Table 1.7: AstroCal system level mass budget by the end of Phase-A.

| | | Contingency (g) | Mass (g) | Percentage Allocation |
|---|---|---|---|---|
| **Subsystems** | ADCS | 61.8 | 1,217.0 | 18% |
| | CDH | 2.7 | 55.7 | 1% |
| | Communications | 12.8 | 344.7 | 5% |
| | Payload | 12.0 | 1,132.3 | 17% |
| | Power | 21.5 | 960.1 | 14% |
| | Structures | 59.5 | 2,857.5 | 43% |
| | Thermal Control | 11.1 | 74.1 | 1% |
| | Wiring Harness | 6.7 | 141.1 | 2% |
| | Integration | 1.8 | 66.5 | 1% |
| | **Total** | **177.8** | **6,716** | **100%** |
| | Target | - | 7,000 | - |
| | Margin | - | 284.4 | 4% |

by the end of Phase-A of AstroCal mission study, there is about 7% mass margin left, which must be increased to 30% by PDR. It must be noted that, although the AstroCal mission is considered to be in its Phase-A, the spacecraft bus design is mature enough that it would not require 30% margin. Therefore, from the beginning, the goal has been to maintain a margin of at least 10% so as to account for the maturity level of the spacecraft bus design and the hardware included.

Moreover, it is important to note that the material selected for the design of structures and payload subsystems is aluminum 6061(density = 2.70 g/cm$^3$) which can be switched to magnesium (density = 1.8 g/cm$^3$) so as to reduce their masses by about 30%.

### 1.5.2 Payload Subsystem Mass Budget

The maximum available mass for AstroCal payload subsystem is 1,000 g as specified in the mission requirements [16]. The overall mass of the payload subsystem by the end of Phase-A is estimated to be 999.0 g, of which 111.9 g is the allocated contingency mass. Therefore, the remaining margin is 1.0 g by the end of Phase-A of the AstroCal mission study.

Fig. 1.18 illustrates each payload instruments mass as a percentage of the overall payload subsystem mass. Detailed payload subsystem mass is presented in Appendix A.5.

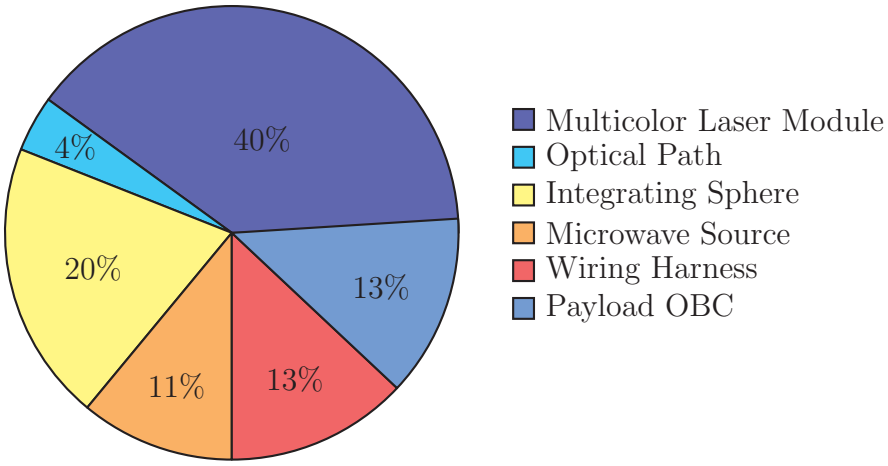


Figure 1.18: Percentage allocated mass of each instrument in the payload subsystem.

## 1.6 Conclusion

### 1.6.1 Summary

In this chapter, the adaptation of the GNB spacecraft to a high-precision astronomical calibration mission is investigated. The mission offers a novel approach for calibration of the ground telescopes that are utilized to study the attenuation of light arriving from distant supernovae due to the Earth's atmosphere, which in turn is studied to determine the amount and characteristics of the dark energy in the universe. The background information regarding the past and present ground telescope calibration techniques is presented. The GNB bus is introduced in details, and is used as the basis for the AstroCal mission study. Minor modifications have been made to the GNB bus so as to eliminate the need for re-designing the spacecraft structures subsystem. Payload instruments are designed from the ground up. Their design is described in details, and where needed, analyses have been performed to prove the feasibility of their concept and design. The proposed design of the multicolor laser module eliminates the needs for optical fibers. Preliminary mass budgets, for the system as a whole and for the payload subsystem, are presented. In order to demonstrate the feasibility of the optical payload, a simple 2-dimensional optics misalignment analysis is presented. The analysis proves that even in the worst case where all misalignments add up in a particular direction away from the optimal path, the laser beam will enter the integrating sphere. The Phase-A of this mission has ended, results of the analyses and the design files have been delivered to the principal investigator. At the moment, the project is waiting for funding.

### 1.6.2 Future Work

Towards the end of the mission study, it was determined that the payload volume available on the GNB form factor may not be sufficiently large to accommodate the AstroCal payload. One particular reason for this is the desire to increase the size of the integrating sphere from 2.0 inches to 4.0 inches, due to limitations in the external surface area provided by the 2-inch sphere. For that, it will be required to step up the spacecraft bus size from GNB to the next available form factor that is offered by SFL, which is the NEMO bus. The NEMO bus is developed based on leveraging the GNB and so many of the analyses performed in this mission study will still apply in case the mission stakeholders decide to switched to the NEMO bus.